Open Access

Research Article

PRNANO

Precis. Nanomed. 2025, 8(1):1414-1430

ANDOVER HOUSE

In vitro study of size-dependent inhibition of human cytochrome P450, (P450-1A2, P450-2A6, P450-2B6, P450-2C8, P450-2E1, P450-2J2, and P450-3A5) by zinc oxide nanoparticles

Lamia Noushin Sadeque Chowdhury[1], Yuh Fen Pung[1], Swee Yong Pung[2], Chin Eng Ong[3], Cin Kong[1], Yan Pan[1*]

[1]*Division of Biomedical Science, School of Pharmacy, University of Nottingham Malaysia, 43500 Semenyih, Malaysia*

[2]*School of Materials and Mineral Resources Engineering, Engineering Campus, University Sains Malaysia, 14300 Nibong Tabal, Penang, Malaysia*

[3]*School of Pharmacy, International Medical University, 57000 Kuala Lumpur, Federal Territory of Kuala Lumpur, Malaysia*

Submitted: November 4, 2024 Accepted: January 19, 2025 Published: February 1, 2025

Graphical Abstract

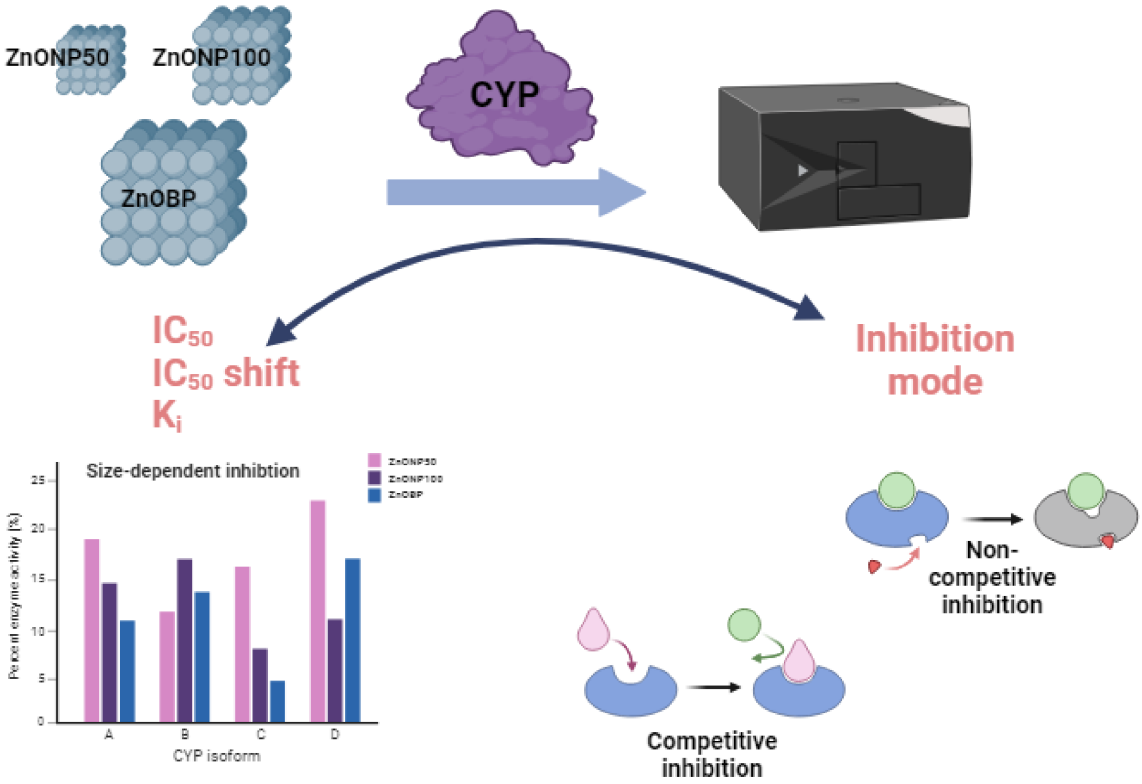

Abstract

Zinc oxide nanoparticles (ZnONPs) are employed widely in various fields. However, these ZnONPs may potentially inhibit enzyme activities. Cytochrome P450 (P450-) isozymes, which play a crucial function in human bio-transforming drugs, can be inhibited by ZnONPs, leading to slower clearance of

* Corresponding Author: panyan1980@hotmail.com, Tel: +6(03) 87253444, Fax: +6(03) 89248018

co-administrated drugs and elevated drug plasma concentrations. This study aimed to reveal the inhibitory effects of the ZnO nano-sized particles (<50 nm [ZnONP50], <100nm [ZnONP100]), and bulk particles (ZnOBP) on human recombinant P450-1A2, P450-2A6, P450-2B6, P450-2C8, P450-2E1, P450-2J2, and P450-3A5 under a size-dependent context. Fluorescence enzymatic assays were carried out to quantify enzyme activities in vitro. The results indicated that ZnO particles inhibited the tested P450- isozymes with varying potencies. ZnONP50 inhibited P450-2B6 and P450- 2E1with K_i values of 20.3µg/mL and 16.6µg/mL following a mixed mode; inhibited P450-2C8 with K_i value of 43.3 µg/mL competitively; inhibited P450-2J2 with K_i values of 8.2 µg/mL and 2. 5µg/mL non-competitively. ZnONP100 inhibited P450-2B6 and P450-2E1 with K_i values of 6.7µg/mL and 40.1µg/mL following mixed mode; inhibited P450-2J2 with K_i value of 20.0µg/mL following mixed or non-competitive mode; inhibited P450-3A5 with K_i value of 0.5µg/mL non-competitively. ZnOBP competitively inhibited the enzymatic activity of P450-2E1 with K_i value of 28.3 µg/mL. The inhibition potency observed for P450-2B6, P450-2J2, and P450-2E1 depended on the size of the ZnO particle. In conclusion, the interactions between ZnONP products and co-administered drugs metabolized by these inhibited P450- isozymes should be further investigated using in vivo models. Additionally, in silico studies are recommended to characterize these interactions at the molecular level.

Keywords: zinc oxide, nanoparticle, cytochrome P450, size-dependent, inhibition

Purpose, Rationale, and Limitations

The widespread use of zinc oxide nanoparticles (ZnONPs) in various industries has raised concerns regarding their potential interactions with drug-metabolizing enzymes, particularly cytochrome P450 (P450) isozymes. These enzymes are critical for metabolizing most clinically relevant drugs, and their inhibition could lead to altered drug pharmacokinetics and potential adverse effects. Despite evidence of nanoparticle-enzyme interactions, the size-dependent effects of ZnONPs on P450 activities remain underexplored. This study investigates the inhibitory potential of ZnONPs of varying sizes (<50 nm, <100 nm, and bulk particles) on key P450 isozymes using *in vitro* enzymatic assays. By elucidating the size-dependent inhibitory patterns, this research provides foundational insights into nanoparticle-enzyme interactions and highlights the implications for nanoparticle safety in biomedical applications.

However, this study is subject to several limitations. Recombinant enzyme systems may not fully replicate the complexity of cellular or *in vivo* environments where factors such as nanoparticle cellular uptake, distribution, and metabolism could influence enzyme inhibition. Additionally, while suitable for high-throughput screening, employing fluorogenic substrates may not entirely represent inhibition dynamics with clinically relevant drug substrates. Future studies employing intact cell models and *in vivo* systems must confirm and expand the findings.

Introduction

Zinc oxide nanoparticles (ZnONPs), which range in size from 1 to 100 nm, are important metal oxide nanoparticles with wide applications due to their favorable physiochemical properties [1]. These properties, including anti-ultraviolet radiation, antimicrobial, and anticancer activities, make ZnONPs suitable for various biomedical applications. Commonly used as inorganic sun blockers, zinc oxide (ZnO) minerals are inert, reducing dermal irritation and penetration [2]. Due to their high biocompatibility, ZnONPs are considered promising candidates for alternative cancer treatments [3]. As ZnONPs are increasingly utilized across different industries, human exposure to these particles is inevitable through inhalation, ingestion, and dermal absorption. Despite their beneficial properties, ZnONPs have shown toxic effects in various organs in several animal models [4]. ZnONP-induced hepatotoxicity is associated with their ability to bind to proteins, induce oxidative stress, and trigger inflammation. These can potentially alter the catalytic activities of cytochrome P450 (P450) enzymes, which are the most important phase I drug-metabolizing enzymes [5], [6].

P450 monooxygenases are membrane-bound hemoproteins that facilitate the biotransformation of xenobiotics (including drugs) and endogenous compounds through oxidation. These enzymes are predominantly expressed at the endoplasmic reticulum of hepatocytes [7]. The en-

zymes from P450-1, P450-2, and P450-3 families are mainly responsible for metabolizing clinical drugs. Fifty-seven P450- isoforms have been identified, and seven (P450-1A2, P450-2A6, P450-2B6, P450-2C8, P450-2E1, P450-2J2, and P450-3A5) are involved in metabolizing 60% of all clinically used drugs [8]. P450-1A2, which accounts for about 15% of P450-mediated drug metabolism, is primarily expressed in the hepatic tissue and metabolizes compounds including clozapine, haloperidol, bilirubin, and estrogens [9]. P450-2A6, involved in 5% of P450-mediated drug metabolism, is found in both hepatic and extrahepatic hepatic tissues and metabolizes coumarin, fadrozole, methoxyflurane, and tegafur [10]. P450-2B6, which handles 12% of P450-mediated drug metabolism, is expressed in the liver and metabolizes bupropion, efavirenz, and ketamine [11]. P450-2C8, responsible for 8% of P450-mediated drug metabolism, is found in the liver, brain, kidney, and gastrointestinal tract, and metabolizes enzalutamide, loperamide, and retinoic acid [12]. P450-2E1, making up 5% of P450-mediated drug metabolism, is primarily in the liver and metabolizes acetaminophen, isoniazid, and ethanol [13]. P450-2J2, which accounts for less than 5% of P450-mediated drug metabolism, is mainly expressed in cardiovascular tissue and metabolizes arachidonic acid, bufuralol, and ebastine [14]. P450-3A5 and P450-3A4, which account for 50% of P450-mediated drug metabolism, are primarily expressed in the liver and share 85% amino acid sequence homology, resulting in similar substrate selectivity. These enzymes metabolize benzodiazepines, erythromycin, and taxol [15], [16]. A significant concern in P450--mediated drug metabolism is the potential for nanoparticle-drug interactions (NDIs). One type of NDI involves the inhibition of P450 isozymes, which may occur when nanoparticles interfere with drug binding to the P450 proteins [17]. This interaction can lead to decreased clearance of the co-administered drug from the patient's system, resulting in subsequent NDIs [18].

Recent literature suggests that various types of nanoparticles (NPs), including ZnONPs, can influence numerous biological factors. NPs have been shown to modulate the catalytic activity of P450- enzymes, increasing the risk of potential toxicity [19], [20], [21]. Additionally, a size-dependent inhibitory effect of several types of NPs on P450- isozymes has been observed [22].

Despite the widespread use of ZnONPs, there is a noticeable gap in research regarding their size-dependent inhibitory potential on P450-isozymes. This study aimed to address this gap by examining the effect of ZnO particles on P450 enzyme activities in a size-controlled context. This study utilized ZnO NPs <50 nm (ZnONP50), ZnO NPs <100nm (ZnONP100), and ZnO bulk particles (ZnOBP) to assess their impact on the enzyme activities of P450-1A2, P450-2A6, P450-2B6, P450-2C8, P450-2E1, P450-2J2, and P450-3A5 and their modes of inhibition.

Experimental Design

This study aimed to explore the fundamental mechanisms of enzyme inhibition by ZnONPs, hypothesizing that ZnONPs exert size-dependent inhibitory effects on human P450 isozymes, potentially altering drug metabolism. To investigate this, an *in vitro* enzyme assay model utilizing recombinant P450 isozymes (Vivid ® CYP450 Screening Kits) was employed. This approach enabled a precise evaluation of ZnONP-induced inhibitory effects on seven key human P450 enzymes (P450-1A2, P450-2A6, P450-2B6, P450-2C8, P450-2E1, P450-2J2, and P450-3A5), which play critical roles in metabolizing clinically relevant drugs. Recombinant human P450 systems were chosen for their suitability in isolating and characterizing direct enzyme interactions, offering distinct advantages over commonly used models such as cell culture systems and *in vivo* studies.

Recombinant human P450 enzymes offer key advantages over cell culture systems by allowing the precise evaluation of individual isoforms without interference from other metabolic pathways, transporters, or cellular processes [23]. Despite being regarded as the “gold standard” by the drug discovery industry, primary hepatocyte cultures are limited by their inconsistent and rare ability to proliferate [24]. Immortalized cell lines, which may exhibit phenotypic drift and altered enzyme expression, recombinant systems ensure consistent and physiologically relevant enzyme activity [25]. Furthermore, the absence of nanoparticle uptake or intracellular trafficking effects simplified the analysis, providing mechanistic clarity. These

recombinant P450 systems are also cost-effective and compatible with high-throughput screening, which has been widely used to evaluate inhibitory effects on P450 enzyme activities [26].

While in vivo models provide insights into tissue-specific nanoparticle distribution and pharmacokinetics, their inherent complexity often complicates the interpretation of direct enzyme-nanoparticle interactions. Species differences in P450 enzyme activities further limit the translatability of in vivo findings to humans [27]. Recombinant systems eliminate these interspecies variations and isolate the enzymatic interactions in a controlled environment, enhancing specificity and mechanistic understanding. Additionally, this approach aligns with the 3Rs framework (Replacement, Reduction, and Refinement), reducing ethical concerns associated with animal use [28].

The use of Vivid® CYP450 fluorogenic substrates adds significant value to this study. These substrates are highly sensitive, soluble, and require minimal solvent use, reducing the risk of solvent-induced inhibition [29]. Importantly, studies have demonstrated that fluorogenic substrates bind to active sites like other conventional substrates, producing comparable results in enzymatic activity and inhibition assays [30]. Their compatibility with high-throughput screening further enhances the efficiency of nanoparticle evaluation, allowing for rapid determination of inhibitory parameters such as IC_{50} and K_i values.

Materials and Methods

Materials and Chemicals

ZnONP50, ZnONP100, and ZnOBP were sourced from Sigma Aldrich (Missouri, USA). Black Costar® 96-well plates were acquired from Thermo Fisher Scientific® (Pennsylvania, USA). Acetonitrile and dimethyl sulfoxide (DMSO) were obtained from Fisher Scientific (Leicestershire, UK). Tris-base was procured from Amresco® LLC (Ohio, USA). Vivid® CYP450 Screening Kits for P450-1A2, P450-2A6, P450-2B6, P450-2C8, P450-2E1, P450-2J2, and P450-3A5 were purchased from Life Technologies™ (California, USA).

Characterization and Preparation of ZnO Particles [31]

The Field Emission Scanning Electron Microscope (FESEM) (Fei Quanta 400F) was employed to capture images of the ZnO particles. The particles were attached to carbon-based double-sided tape to prepare the samples, which were then affixed to an electron microscope stub. Magnifications ranged from 50,000X to 240,000X, with the in-lens detector operating at 20.00 kV to capture the high-resolution secondary electron images. The imaging parameters included a 10.0-10.3 mm working distance and an aperture size from 2 µm to 500 nm. Moreover, Energy Dispersive X-ray Spectroscopy (EDX) (Oxford-Instruments INCA 400 with X-Max Detector) was utilized to acquire elemental maps of all three ZnO particle sizes, measuring the elemental composition of carbon, oxygen, zinc, and aluminum. The X-ray detectors for all ZnO particles were positioned at a tilt of 0.0°, an elevation of 35.0°, and an azimuth of 0.0°, with the beam's accelerating voltage maintained at 20.00 kV. The Malvern Zetasizer Nano ZS (Malvern Instruments, UK) was used to measure the hydrodynamic size and zeta potential of ZnO nanoparticles in MilliQ water.

To avoid contamination and to minimize aggregation of the bulk/nano-sized powder, ZnONP50, ZnONP100, and ZnOBP were freshly prepared for each assay. DMSO was employed as a solvent to achieve the initial concentration of 10 mg/mL for each type of ZnO particle, followed by 30 minutes' solution at 30°C to obtain the optimal dispersion stability.

Generation of Standard and Time Curves

To establish standard curves, fluorescence readings (FRU) measured using Vivid® Blue Standard (3-cyano-7-hydroxycoumarin) prepared in Buffers I, II, and III, Vivid® Cyan Standard (7-hydroxy-4-trifluoromethylcoumarin) in Buffer II, and Vivid® Green Standard (fluorescein) in Buffer II against a spectrum of concentrations (500, 250, 125, 62.5, 31.25, 15.6, 7.81, 3.905, and 0 nM) were plotted. The derived equations from the standard curves were subsequently used to quantify the fluorometric metabolites produced in later assays. Additionally, to determine the optimal fluorometric metabolite production by each P450 isozyme, we conducted time curve experiments

with incubation periods of 0, 5, 10, 20, 30, 60, 90, 120, 180, and 240 minutes. The optimal reaction time for respective P450 enzyme assay was determined based on the linear phase of the curve.

Measurement of P450 Isozyme Activity

The catalytic activities of targeted P450 isoforms, including P450-1A2, P450-2A6, P450-2B6, P450-2C8, P450-2E1, P450-2J2, and P450-3A5, were measured employing the corresponding Vivid® CYP450 Screening Kits following the protocol of endpoint mode [32]. The assays were performed in 96-well plates at room temperature (25-27°C). Each reaction well contained 40 µL of the recommended Vivid® CYP450 Reaction Buffer (Buffer I - P450-1A2/P450-2B6/P450-3A5; Buffer II - P450-2A6/P450-2C8/P450-2J2; Buffer III - P450-2E1) and a master pre-mix (50 µL) containing P450-450 BACULOSOMES® Plus Reagent, Vivid® Regeneration System, and Vivid® CYP450 Reaction Buffer. A pre-incubation of 30 minutes was carried out, followed by initiating the reactions with the addition of 10 µL of a mixture of the respective Vivid® Substrate and 0.03 mM NADP+ per well, using Vivid® BOMCC (7-benzyloxymethyloxy-3-cyanocoumarin) for P450-2B6/P450-3A5, Vivid® CC (3-cyano-coumarin) for P450-2A6, Vivid® DBOMF (di-(benzyl-O-methyl)-fluorescein) for P450-2C8, Vivid® EOMCC (7-ethoxy-methyloxy-3-cyanocoumarin) for P450-1A2/P450-2E1, and Vivid® MOBFC (7-P-methoxy-benzyloxy-4-trifluoro-coumarin) for P450-2J2. The 100 µL reaction mixture was incubated for 120 minutes, and tris-base solution (50 µL, 0.5 M) was added to stop the reaction. The catalytic activities of the P450- isozymes quantified using the Varioskan Flash Plate Reader (Thermo Fisher Scientific®, Massachusetts, USA) at excitation/emission wavelengths of 415/460 nm (P450-1A2/P450-2A6/P450-2B6/P450-2E1/P450-3A5), 490/520 nm (P450-2C8), and 415/520 nm (P450-2J2). Table S1 (supplementary information) summarises all final concentrations of reagents used in these P450 enzyme assays.

Table 1. Assay Conditions to Determine K_i and Mode of Inhibition

P450 Isozyme	ZnO Particle*	ZnO Particle Concentration (µg/mL)	Vivid® Substrate Concentration (µM)
2B6	ZnONP50	50, 25, 12.5, 6.25, 0	BOMCC – 2.5, 5, 10, 20
	ZnONP100	50, 25, 12.5, 6.25, 0	
2C8	ZnONP50	50, 25, 12.5, 6.25, 0	DBOMF – 2.5, 5, 10, 20
2E1	ZnONP50	50, 25, 12.5, 6.25, 0	EOMCC – 10, 20, 40, 80
	ZnONP100	100, 50, 25, 12.5, 0	
	ZnOBP	50, 25, 12.5, 6.25, 0	
2J2	ZnONP50	50, 25, 12.5, 6.25, 0	MOBFC – 2.5, 5, 10, 20
	ZnONP100	100, 50, 25, 12.5, 0	
3A5	ZnONP50	100, 50, 25, 12.5, 0	BOMCC – 2.5, 5, 10, 20
	ZnONP100	50, 25, 12.5, 6.25, 0	

Reversible Inhibition Studies with ZnO Particles

To prepare stock solutions of ZnONP50, ZnONP100, and ZnOBP, each ZnO powder was dispersed using DMSO to achieve a 10mg/mL concentration. The reversible inhibition assays followed the conditions outlined in the earlier section, including the respective ZnO particle solutions in 40 µL of Vivid® CYP450 Reaction Buffer [32]. This resulted in a 0 to 1000 µg/mL concentration after performing two-fold serial dilutions. The percentage of control activity (%) at a defined concentration of ZnO particle investigated was calculated by dividing the enzymatic activity by the activity determined using the solvent control (where the ZnO particle solution was replaced with

DMSO) and multiplying the result by 100. These values (percent control activity) were plotted against the ZnO particles log concentrations to generate IC_{50} curves. For ZnO particles exhibiting significant inhibition of P450 isozymes (IC_{50} < 100 µg/mL), the inhibition constant (K_i) and inhibition mode were further characterized. These were done by incubating various concentrations of ZnO particles with different concentrations of Vivid® Substrates, as described in Table 1.

Irreversible Inhibition Studies with ZnO Particles

Irreversible inhibition, also known as time-dependent inhibition (TDI), was also evaluated following similar steps of reversible P450-inhibition assays with some modifications. The TDI assays included two experimental conditions: one with a 30-minute incubation with NADPH (NADPH +) and one without NADPH (NADPH -) [32]. For (NADPH +), Vivid® NADP+ was added to the master pre-mix as described above, and the substrate mixture only contained Vivid® Substrate in the respective Vivid® CYP450 Reaction Buffer. For (NADPH -), the assay conditions were the same as described in Section 2.3. IC_{50} values obtained were used to derive the IC_{50} shift ratio, and a ratio of more than two indicated significant TDI, categorizing the ZnO particle as an irreversible inhibitor.

Data Analysis

IC_{50} values were acquired through a nonlinear regression model employing GraphPad Prism 9.4.1 for Mac (GraphPad Software, La Jolla, California, USA). Standard curve equations were used to quantify the formations of metabolites. These were subsequently applied to calculate the reaction velocities, representing P450-enzyme activities. Lineweaver-Burk plots were generated in Microsoft Excel to graphically determine the mode of inhibition based on the intercept patterns. The slopes of curves from Lineweaver-Burk plots were plotted against the concentrations of ZnO particles (µg/mL) to establish a secondary plot, from which the K_i values were determined.

Results

Characterization of ZnO Particles

Table 2 summarizes the physical and surface properties of ZnO nanoparticles and bulk particles, including the primary size, hydrodynamic size, and zeta potential.

Table 2. Summary of Physical and Surface Properties of ZnO Nano and Bulk Particles

	Primary size (nm)	Hydrodynamic size (nm)	Zeta Potential (mV)
ZnO <50 nm	38.53 ± 1.7	175.4 ± 0.44	26.23 ± 0.13
ZnO <100 nm	80.98 ± 3.7	546.6 ± 5.92	20.87 ± 0.33
Bulk ZnO	223.17 ± 13.1	1566 ± 13.58	-9.78 ± 0.91

ZnONP50 showed irregular shapes, and the primary sizes were determined within a range of 38.59 to 50.24 nm, as depicted in Figure 1 A1 and A2. Elemental analysis indicated the presence of aluminum (2.50%), carbon (7.17 %), oxygen (25.19%), and zinc (65.14%) as illustrated in Figure 1 A3.

ZnONP100 primarily exhibited a cylindrical shape with sizes of 43.13 to 94.11 nm, as shown in Figures 1 B1 and B2. Elemental analysis revealed the presence of carbon (8.53%), oxygen (16.06%), and zinc (75.41%), which was validated by elemental mapping, as shown in Figure 1 B3.

ZnOBP particles lacked a uniform shape and varied in size from 119.9 to 259.8 nm, as indicated in Figures 1 C1 and C2. Elemental analysis showed they contained carbon (20.72%), oxygen (23.52%), and zinc (55.76%), as indicated in Figure 1 C3. The peaks for carbon, oxygen, and zinc were at 0.3, 0.5, and 1.0, 8.6, and 9.8 keV, respectively.

All ZnO particles, including aluminum, exhibited multiple signal peaks corresponding to known ZnO absorptions. The absence of extraneous peaks confirmed the purity of ZnONP50, ZnONP100, and ZnOBP [33], [34].

A1

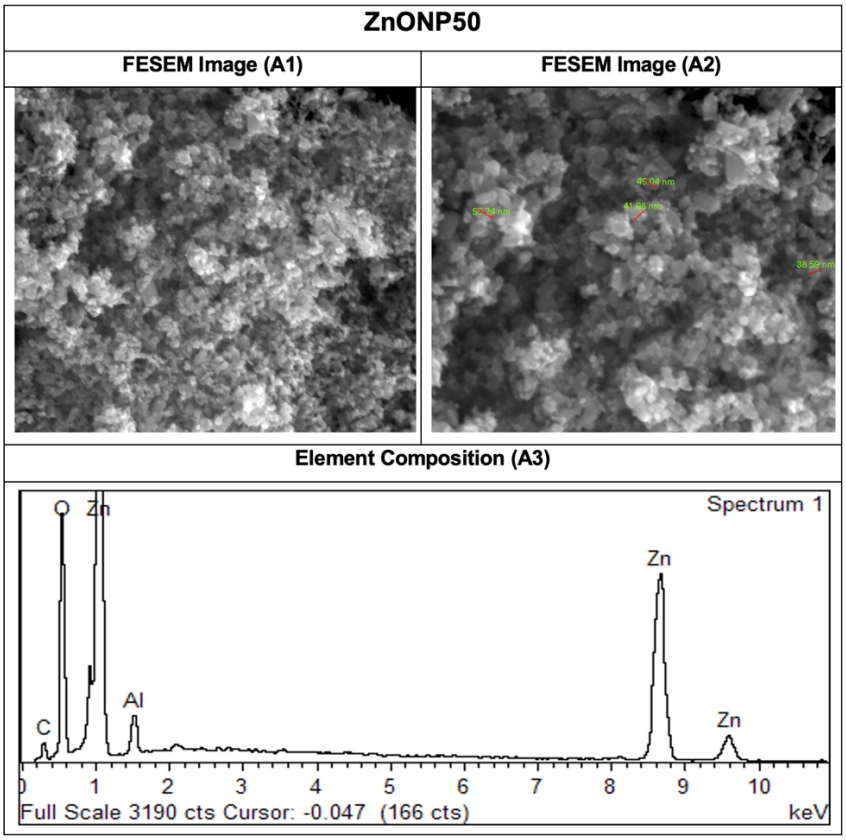

A2

A3

B1

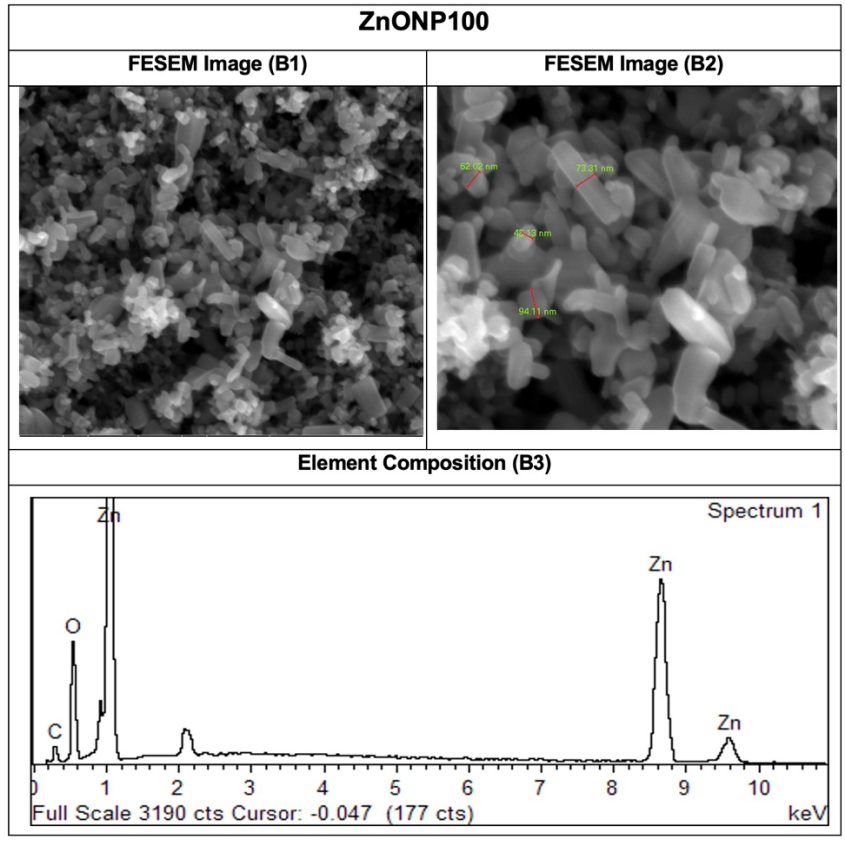

B2

B3

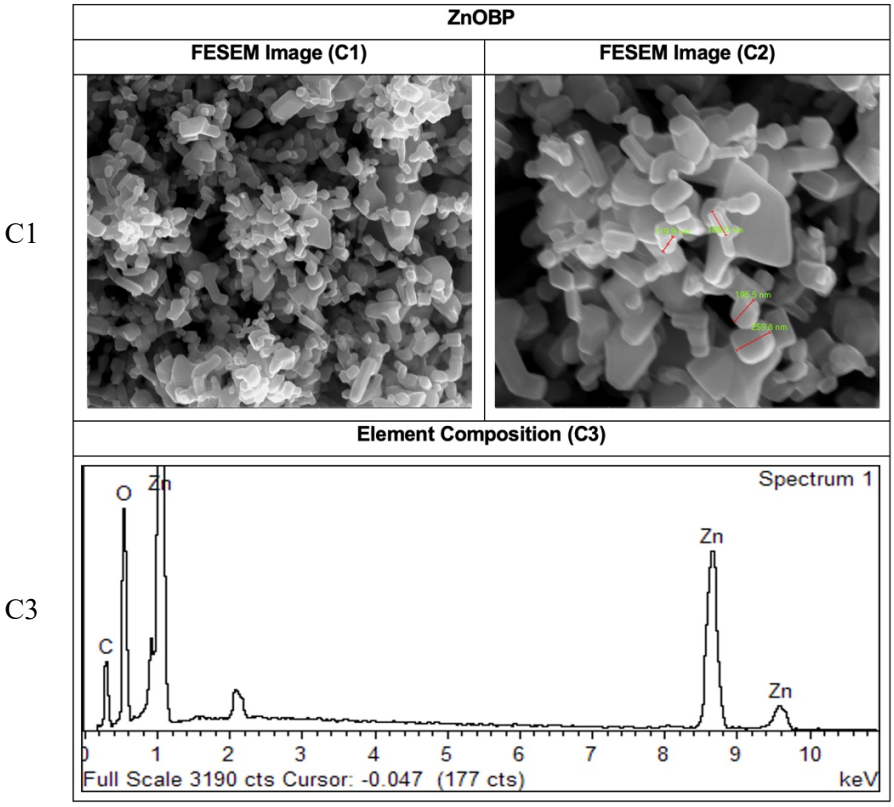

Figure 1. Characterization of ZnO particles: ZnONP50, A1) shape, A2) size (FESEM,120X-200X) and A3) EDX; ZnONP100, B1) shape, B2) size (FESEM,120X-240X) and B3) EDX; ZnOBPs, C1) shape, C2) size (FESEM, 50X-120X) and C3) EDX.

Standard and Time Curves

The standard curve equations for the blue standard (3-cyano-7-hydroxycoumarin) in Buffer I, 0.5X Buffer II, and Buffer III were determined as y = 0.0065x + 0.0329, y = 0.0054x – 0.0046, and y = 0.006x – 0.0177, respectively. The equation for the cyan standard (7-hydroxy-4-trifluoromethylcoumarin) in Buffer II was y = 0.0002x – 0.0094. The green standard (fluorescein) in Buffer II was described by the equation y = 0.0075x + 0.0026.

After 120 minutes, the post-linear phase for all investigated P450 isoforms was achieved, where the respective enzymatic activities reached a plateau, as depicted in Figure 2. Consequently, 120 minutes was selected as the incubation duration for the P450 enzyme assays in this study.

Reversible Inhibition Potencies (IC_{50} and K_i) and Inhibition Modes

IC_{50} (defined as the half-maximal inhibitory concentration) values for P450-1A2, P450-2A6, P450-2B6, P450-2C8, P450-2E1, P450-2J2, and P450-3A5 in the presence of ZnONP50, ZnONP100, and ZnOBP were assessed (see Figures S1-S7 in supplementary information). This study defined significant inhibition by IC_{50} values below 100 µg/mL. To determine whether inhibition occurred in a size-dependent manner, the remaining enzymatic activities (percent control activity) were compared with a concentration of 100 µg/mL of ZnONP50, ZnONP100, and ZnOBP (Figure 3). The inhibition potentises on P450-2A6, P450-2C8, P450-2E1, and P450-3A5 by ZnONP50, ZnONP100 and ZnOBP following a ZnONP50>ZnONP100>ZnONPBP size-dependent trend. Figure S8 demonstrates Lineweaver-Burk and secondary plots for each P450 isozyme incubated with the respective ZnO particle. The mode of inhibition and the K_i values determined from these plots were summarized in Table 3.

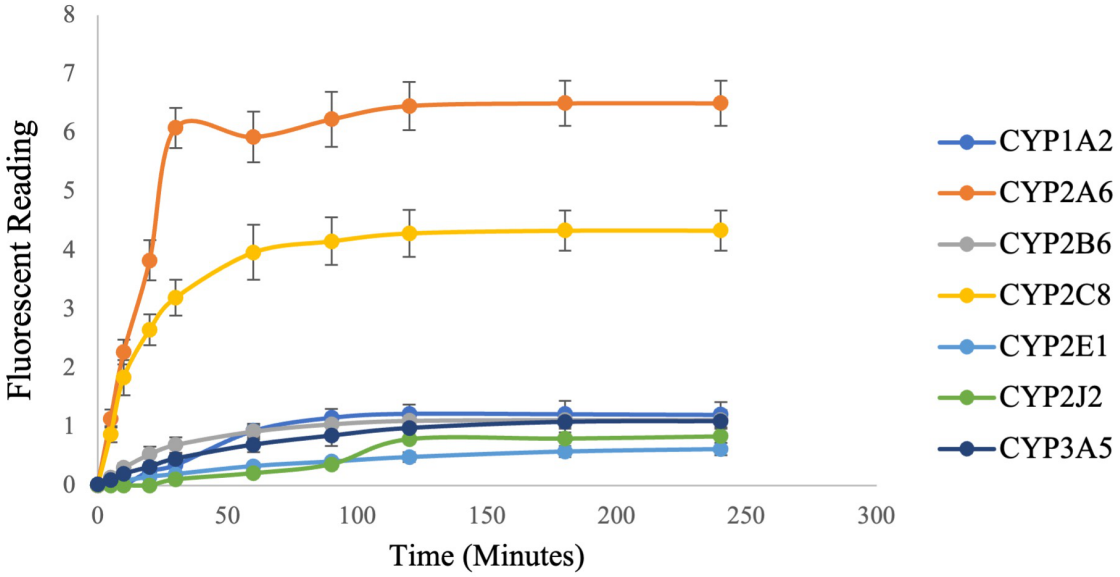

Figure 2. *Time curves of P450 isozymes (P450-1A2, P450-2A6, P450-2B6, P450-2C8, P450-2E1, P450-2J2, and P450-3A5) plotted against incubation periods (5-240 minutes) using fluorescent readings of oxidising Vivid® Substrates. Each point represents mean ± SD (n=3).*

Firstly, these results showed that ZnONP50 inhibited P450-2B6 (IC_{50}=8.1 µg/mL and K_i=20.3 µg/mL) and P450-2E1 (IC_{50}= 4.9 µg/mL and K_i=16.6 µg/mL) via a mixed mode; P450-2C8 (IC_{50}= 10.2 µg/mL and K_i=43.3 µg/mL) via a competitive mode; P450-2J2 (IC_{50}= 2.1 µg/L and K_i=8.2 µg/mL) and P450-3A5 (IC_{50}=21.3 µg/mL and K_i=2.5 µg/mL) non-competitively.

Table 3. Summary of Ki Values and the Modes of Inhibition

P450 Isozyme	ZnO Particle	Inhibition Constant (K_i) (µg/mL)	Mode of Inhibition
2B6	ZnONP50	20.3	Mixed
	ZnONP100	6.7	Mixed
2C8	ZnONP50	43.3	Competitive
2E1	ZnONP50	16.6	Mixed
	ZnONP100	40.1	Mixed
	ZnOBP	28.3	Competitive
2J2	ZnONP50	8.2	Non-competitive
	ZnONP100	20.0	Mixed or Non-competitive
3A5	ZnONP50	2.5	Non-competitive
	ZnONP100	0.5	Non-competitive

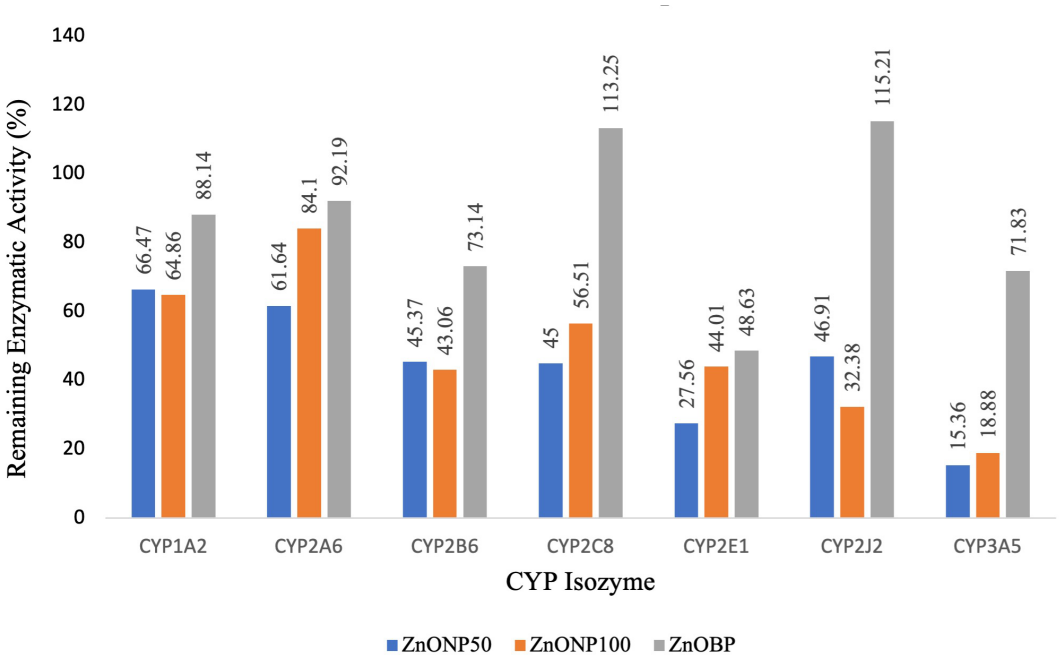

Figure 3. *Evaluation of the size-dependent inhibition of P450 isozymes upon exposure to 100μg/mL of ZnONP50, ZnONP100, and ZnOBP.*

These results show that ZnONP50 inhibits P450-2B6 (IC_{50}=8.1 μg/mL and K_i=20.3 μg/mL) and P450-2E1 (IC_{50}= 4.9 μg/mL and K_i=16.6 μg/mL) via a mixed mode; P450-2C8 (IC_{50}= 10.2 μg/mL and K_i=43.3 μg/mL) via a competitive mode; while P450-2J2 (IC_{50}= 2.1 μg/L and K_i=8.2 μg/mL) and P450-3A5 (IC_{50}=21.3 μg/mL and K_i=2.5 μg/mL) does it non-competitively.

Secondly, ZnONP100 inhibited P450-2B6 (IC_{50}=8.4 μg/mL and K_i=6.7 μg/mL) and P450-2E1 (IC_{50}=36.1 μg/mL and K_i=40.1 μg/mL) through a mixed manner; P450-2J2 (IC_{50}= 23.3 μg/mL and K_i=20.0 μg/mL) by a mixed or a non-competitive mode; P450-3A5 (IC_{50}:=7.9 μg/mL and K_i=0.5 μg/mL) competitively. Finally, ZnOBP competitively inhibited P450-2E1 (IC_{50}=16.3 μg/mL and K_i=28.3 μg/mL).

Table 4. Determinations of IC_{50} Shifts to Detect the Presence of TDI

P450 Isozyme	ZnO Particles	IC_{50} without NADPH (μg/mL)	IC_{50} with NADPH (μg/mL)	IC_{50} shift
2B6	ZnONP50	17.6	3.67	4.80*
	ZnONP100	10.99	10.47	1.05
2C8	ZnONP50	35.34	12.44	2.84*
2E1	ZnONP50	7.23	15.33	0.47
	ZnONP100	9.42	4.93	1.91
	ZnOBP	0.33	0.27	1.22
2J2	ZnONP50	39.45	18.02	2.19*
	ZnONP100	6.91	4.27	1.62
3A5	ZnONP50	22.14	15.19	1.46
	ZnONP100	14.63	11.81	1.24

*IC_{50} shift > 2, suggesting the presence of TDI by ZnONP on P450 activity

Time-Dependent Inhibition (TDI)

IC_{50} value of incubation without NADPH (NADPH -) over IC_{50} value with NADPH (NAPDH +) was calculated to obtain IC_{50}-shift. Figures S9-S13 in the supplementary information showed the IC_{50}-shift curves, and the IC_{50} shift ratios were presented in Table 4. An IC_{50} shift greater than two-fold defined a potential TDI. The results suggested ZnONP50 inhibited P450-2B6, P450-2C8, and P450-2J2 following TDI mode

Discussion

ZnONPs are valued for their UV-blocking properties, hence, widely employed in cosmetics and sunscreens. However, they may enter the human body following dermal absorption or incidental ingestion, leading to toxicities in various organs and systems. Our earlier study has reported an update on the toxicities of ZnONPs using *in vivo* animal models [4]. Once ZnONPs are absorbed, their potential to inhibit key drug-metabolizing enzymes such as P450 isozymes raises concerns. Enzyme inhibition could alter the metabolism of concomitantly administered drugs, leading to altered pharmacokinetics, potential drug accumulation, or toxicity [35]. This highlights the importance of characterizing ZnONP formulations for efficacy and safety, particularly in terms of potential interactions with drug-metabolizing enzymes [36].

NPs possess distinct characteristics compared to their BP equivalents, particularly in size and surface area-to-volume ratio, which enhance their dispersion and transparency properties [37]. Moreover, NPs have a more significant number of surface atoms, increasing their reactivity and responsiveness [38]. These physicochemical attributes significantly influence the behavior, bio-distribution, and toxicological effects of NPs. Since size and chemical composition are critical factors affecting the toxicity and inhibitory potential of NPs, this study employed ZnOBP as a benchmark to explore the size-specific inhibitory effects of ZnONPs [39].

The average particle sizes of ZnOBP tested in this study were determined to be 223.17 ± 13.1 nm (n=4), classifying them as bulk-sized particles. In contrast, the average particle sizes of ZnONP100 and ZnONP50 were measured at 80.98 ± 3.7 nm (n=4) and 38.53 ± 1.7 nm (n=4), respectively, aligning with the typical size range of nanoparticles. This confirms their classification as nanoparticles, as defined by their size [40]. Furthermore, the compositional purity of all three sizes of ZnO particles was verified, as no unwanted elements were detected [41]. However, the hydrodynamic size measured by dynamic light scattering revealed a marked increase in all three types of ZnO particles (Table 2). Smaller ZnO particles (ZnONP50 and ZnONP100) demonstrated positive zeta potentials, whereas the bulk ZnO particle (ZnOBP) exhibited a negative zeta potential. The positive surface charge observed in smaller nanoparticles is likely due to hydroxyl group adsorption or stabilization in aqueous media, which promotes particle dispersion and reduces aggregation. Conversely, the negative zeta potential of the bulk particle indicates surface charge inversion, potentially caused by different stabilizing conditions or weaker interactions with the dispersion medium. This shift in zeta potential can result in enhanced aggregation, as observed in the significantly larger hydrodynamic size of ZnOBP. Thus, the zeta potentials of these ZnO particles play a crucial role in determining their hydrodynamic sizes, reflecting their stability and interaction within the colloidal system [42], [43].

The reversible inhibition of each ZnO particle on P450 isozyme activity was assessed by determining IC_{50} and K_i values. IC_{50} indicates the concentration of inhibitor needed to reduce the enzyme activity by 50%, while K_i reflects the inhibitor's potency and aids in categorizing the type of reversible inhibition graphically [44], [45]. A rather robust approach was adopted to classify the inhibitory potencies into weak (IC_{50} or $K_i \geq 10$ µg/mL), moderate (IC_{50} or K_i within 1 to 10 µg/mL), and potent (IC_{50} or $K_i \leq 1$ µg/mL) [46].

As depicted in Figure S8, ZnO particles inhibited P450 enzymes through competitive, non-competitive, or mixed modes. Under a competitive inhibition, the ZnO particle binds to the same active site of the P450 isozyme as the substrate binds, preventing metabolite formation. To counteract competitive inhibition, increasing the substrate concentration is a validated approach. This increase can restore the enzyme's metabolic function by overcoming the inhibitory effect of the ZnO particle [47]. In contrast, a non-competitive inhibition results when the ZnO particle attaches to an allosteric site on the

P450 isozyme rather than the active site. This interaction causes a conformational alteration of the P450 active site, which interferes with the binding affinity of the substrate. Unlike competitive inhibition, increasing the substrate concentration does not counteract non-competitive inhibition [48]. Mixed-type inhibition occurs when an inhibitor can bind to the enzyme's active site and the enzyme-substrate complex, but not with equal affinity. This type of inhibition involves competitive and non-competitive inhibition [49]. Reversible inhibition can lead to slower clearance of drugs and hence increased bioavailability. This heightened bioavailability can cause several adverse outcomes, including reduced efficacy, adverse drug reactions, and potential toxicity [50].

As shown in Figure 3, size-dependent inhibition was observed, and similar observations were reported by studies involving other NPs, which also found that smaller NPs tend to produce stronger reversible inhibition on various P450 isozymes. Although size-dependent inhibition was not observed for P450-1A2, P450-2B6, and P450-2J2, ZnOBP generally exhibited lower inhibitory potencies than ZnONPs. ZnONP100 demonstrated comparable (for P450-1A2 and P450-2B6) or slightly higher (P450-2J2) inhibitory effects than ZnONP50. This disparity in inhibitory effects may be due to the larger size and reduced surface area-to-volume ratio of ZnOBP, which potentially limits its reactivity and interaction with the active sites or allosteric sites of the P450- enzymes. In contrast, the smaller ZnONPs, with their higher surface area-to-volume ratio, likely have increased reactivity, allowing for more effective interactions and inhibition of the P450 enzymes. This suggests that the physical characteristics of the particles play a significant role in their ability to inhibit P450 enzyme activity [51], [52].

Inhibition of P450 isozymes can also occur irreversibly, known as mechanism-based inhibition or TDI [53]. According to the results in Table 4, ZnONP50 was identified as an irreversible inhibitor of P450-2B6, P450-2C8, and P450-2J2, with fold-shifts exceeding 2. Mechanism-based inhibitors are of more significant clinical concern because their effects are often more profound and longer-lasting than those of reversible inhibitors. TDIs arise from non-covalent tight binding or irreversible covalent binding, leading to a loss of enzymatic function. The inhibitory effect increases when the P450 is pre-incubated with the testing compound before the substrate is added to a TDI assay. Additionally, irreversible inhibition remains even after removing the inhibitor [54]. Therefore, TDIs involving P450-2B6, P450-2C8, and P450-2J2 with ZnONP50 may result in heightened systemic exposure to co-administered drugs.

Understanding the interaction mechanisms between ZnO particles and P450 isozymes involves two hypotheses. Firstly, it emphasizes the role of oxygen molecules in ZnO particles. Oxygen molecules impart a negative surface charge to ZnO particles, enabling them to form weak hydrogen bonds. This allows both covalent and non-covalent interactions with biomolecules [55], [56]. The EDX analysis confirmed a high oxygen content in all ZnO particle sizes, with ZnONP50 exhibiting the highest percentage. This mechanism aligns with our findings, as P450-2B6, P450-2C8, P450-2E1, and P450-3A5 inhibition was size-dependent, showing stronger inhibition with smaller particles. The second mechanism focuses on the dissolution of Zn^{2+} ions. The high surface area of ZnONPs means a significant proportion of ZnO molecules are exposed on the particle surface. In the active state, oxygen atoms on the ZnO surface bind hydrogen molecules to form hydrogen bonds, resulting in Zn^{2+} ions dissolution ($ZnO + 2H^{+} \rightarrow Zn^{2+} + H_2O$) [57]. The rate of Zn^{2+} ion release is inversely related to particle size, suggesting that smaller ZnO particles, like ZnONP50, have a faster release and dissociation rate than larger particles [58]. This mechanism may explain the overall more substantial inhibitory potential observed for ZnONP50 compared to ZnONP100 and ZnOBP.

This research has highlighted the inhibitory effects of different sizes of ZnO particles, particularly the smallest variant, ZnONP50, on the activity of P450-2B6, P450-2C8, P450-2E1, P450-2J2, and P450-3A5 enzymes. Such inhibition can have significant clinical implications for drugs metabolized by these enzymes. For example, efavirenz, an HIV treatment metabolized by P450-2B6, has a narrow therapeutic window. Inhibiting P450-2B6 can lead to higher plasma levels of efavirenz, causing adverse effects like liver damage, neurotoxicity, and drug resistance [59]. Another example is

paclitaxel, a chemotherapy drug metabolized by P450-2C8. Inhibiting P450-2C8 can reduce the drug's effectiveness and lead to side effects such as nausea, inflammation, and muscle pain [60]. Additionally, tacrolimus, an immunosuppressant used in organ transplant patients and metabolized by P450-3A5, has a narrow therapeutic range. Inhibiting P450-3A5 can increase tacrolimus levels in the blood, leading to neurotoxicity, kidney damage, and organ rejection [15].

This study provides foundational insights into the size-dependent inhibitory effects of ZnONPs on human P450 enzymes; however, it is not without limitations. The use of recombinant P450 enzymes, while highly specific and reproducible, does not fully capture the complexity of cellular and systemic environments where factors such as nanoparticle uptake, intracellular trafficking, and metabolic interactions play a role. Additionally, though practical and efficient, fluorogenic substrates may not fully replicate inhibition profiles observed with clinically relevant drug substrates. Future studies should incorporate cell-based assays, such as those using primary human hepatocytes, to evaluate these interactions under more physiologically relevant conditions. Furthermore, pharmacometrics modeling and *in vivo* animal studies would be valuable for determining whether the observed *in vitro* inhibition occurs at drug exposure levels pertinent to clinical or preclinical settings. These efforts will help translate current findings into actionable insights for drug development and safety assessment.

Conclusion

In conclusion, this study demonstrates that smaller ZnO NPs, particularly ZnONP50, exhibit more potent inhibitory effects on key P450 enzymes (P450-2B6, P450-2C8, P450-2E1, P450-2J2, and P450-3A5) compared to larger particles. To further explore the inhibitory mechanism of ZnO particles on P450-catalytic activities, conducting in silico studies to model the interaction at the atomic level is recommended. This approach will help characterize how ZnO behaves near the enzyme's active site, providing insights into the underlying biochemical mechanism. Additionally, in vivo investigations using animal models or human subjects should be considered to validate these inhibitory effects of ZnONPs on P450. If these effects are confirmed, caution should be taken when drugs metabolized by affected P450- enzymes are co-administered with ZnO NP products.

Acknowledgments

Author Contributions: Conceptualization: Yan Pan, Yuh Fen Pung, Cin Kong, Swee Yong Pung; Methodology: Yan Pan, Chin Eng Ong, Swee Yong Pung; Data Collection: Lamia Noushin Sadeque Chowdhury; Data Analysis: Lamia Noushin, Sadeque Chowdhury, Yan Pan; Writing Original Draft: Lamia Noushin, Sadeque Chowdhury; Writing, Review, and Editing: Yan Pan, Cin Kong; Supervision: Yan Pan, Yuh Fen Pung; Funding Acquisition: Yan Pan.

Funding: The authors express gratitude to the Fundamental Research Grant Scheme (FRGS) the Ministry of Higher Education Malaysia awarded to provide financial support in this study [grant number: FRGS/1/2019/SKK10/UNIM/02/1].

Conflicts of Interest: The authors declare no conflict of interest. The funders had no role in the study's design, data collection, analysis, interpretation, manuscript writing, or decision to publish the results. For a written statement, please contact the journal office editor@precisionnanomedicine.com.

Quote this article as Chowdhury, Lamia, Yuh Fen Pung, Swee Yong Pung, Chin Eng Ong, Cin Kong, and Yan Pan. 2025. "In Vitro Study of Size-Dependent Inhibition of Human Cytochrome P450 (P450) P450-1A2, P450-2A6, P450-2B6, P450-2C8, P450-2E1, P450-2J2, and P450-3A5 by Zinc Oxide Nanoparticles (ZnONPs)."*Precis. Nanomed.*, February, 1414–30, https://doi.org/10.33218/001c.129234.

References

[1] K. A. Altammar, "A review on nanoparticles: characteristics, synthesis, applications, and challenges," *Front. Microbiol.*, vol. 14, p. 1155622, Apr. 2023, doi: 10.3389/fmicb.2023.1155622.

[2] C. Antoniou, M. Kosmadaki, A. Stratigos, and A. Katsambas, "Sunscreens – what's important to know," *Acad Dermatol Venereol*, vol. 22, no. 9, pp. 1110–1119, Sep. 2008, doi: 10.1111/j.1468-3083.2007.02580.x.

[3] Y. Zhang, T. Nayak, H. Hong, and W. Cai, "Biomedical Applications of Zinc Oxide Nanomaterials," *CMM*, vol. 13, no. 10, pp. 1633–1645, Nov. 2013, doi: 10.2174/15665240136661311111130058.

[4] C. L. Chong *et al.*, "Current Updates On the In vivo Assessment of Zinc Oxide Nanoparticles Toxicity Using Animal Models," *BioNanoSci.*, vol. 11, no. 2, pp. 590–620, Jun. 2021, doi: 10.1007/s12668-021-00845-2.

[5] L. M. De Jong, W. Jiskoot, J. J. Swen, and M. L. Manson, "Distinct Effects of Inflammation on Cytochrome P450 Regulation and Drug Metabolism: Lessons from Experimental Models and a Potential Role for Pharmacogenetics," *Genes*, vol. 11, no. 12, p. 1509, Dec. 2020, doi: 10.3390/genes11121509.

[6] M. I. Luster, P. P. Simeonova, R. M. Gallucci, A. Bruccoleri, M. E. Blazka, and B. Yucesoy, "Role of inflammation in chemical-induced hepatotoxicity," *Toxicology Letters*, vol. 120, no. 1–3, pp. 317–321, Mar. 2001, doi: 10.1016/S0378-4274(01)00284-3.

[7] K. Gerth, S. Kodidela, M. Mahon, S. Haque, N. Verma, and S. Kumar, "Circulating Extracellular Vesicles Containing Xenobiotic Metabolizing CYP Enzymes and Their Potential Roles in Extrahepatic Cells Via Cell–Cell Interactions," *IJMS*, vol. 20, no. 24, p. 6178, Dec. 2019, doi: 10.3390/ijms20246178.

[8] U. M. Zanger and M. Schwab, "Cytochrome P450 enzymes in drug metabolism: Regulation of gene expression, enzyme activities, and impact of genetic variation," *Pharmacology & Therapeutics*, vol. 138, no. 1, pp. 103–141, Apr. 2013, doi: 10.1016/j.pharmthera.2012.12.007.

[9] F. Fekete, K. Mangó, A. Minus, K. Tóth, and K. Monostory, "CYP1A2 mRNA Expression Rather than Genetic Variants Indicate Hepatic CYP1A2 Activity," *Pharmaceutics*, vol. 14, no. 3, p. 532, Feb. 2022, doi: 10.3390/pharmaceutics14030532.

[10] V. M. Kramlinger, L. B. Von Weymarn, and S. E. Murphy, "Inhibition and inactivation of cytochrome P450 2A6 and cytochrome P450 2A13 by menthofuran, β-nicotyrine and menthol," *Chemico-Biological Interactions*, vol. 197, no. 2–3, pp. 87–92, May 2012, doi: 10.1016/j.cbi.2012.03.009.

[11] I. M. Langmia, K. S. Just, S. Yamoune, J. Brockmöller, C. Masimirembwa, and J. C. Stingl, "CYP2B6 Functional Variability in Drug Metabolism and Exposure Across Populations—Implication for Drug Safety, Dosing, and Individualized Therapy," *Front. Genet.*, vol. 12, p. 692234, Jul. 2021, doi: 10.3389/fgene.2021.692234.

[12] C. L. Aquilante, M. Niemi, L. Gong, R. B. Altman, and T. E. Klein, "PharmGKB summary: very important pharmacogene information for cytochrome P450, family 2, subfamily C, polypeptide 8," *Pharmacogenetics and Genomics*, vol. 23, no. 12, pp. 721–728, Dec. 2013, doi: 10.1097/FPC.0b013e3283653b27.

[13] J. Hakkola, J. Hukkanen, M. Turpeinen, and O. Pelkonen, "Inhibition and induction of CYP enzymes in humans: an update," *Arch Toxicol*, vol. 94, no. 11, pp. 3671–3722, Nov. 2020, doi: 10.1007/s00204-020-02936-7.

[14] X. Tian *et al.*, "The development of novel cytochrome P450 2J2 (CYP2J2) inhibitor and the underlying interaction between inhibitor and CYP2J2," *Journal of Enzyme Inhibition and Medicinal Chemistry*, vol. 36, no. 1, pp. 737–748, Jan. 2021, doi: 10.1080/14756366.2021.1896500.

[15] A. R. Khan, A. Raza, S. Firasat, and A. Abid, "CYP3A5 gene polymorphisms and their impact on dosage and trough concentration of tacrolimus among kidney transplant patients: a systematic review and meta-analysis," *Pharmacogenomics J*, vol. 20, no. 4, pp. 553–562, Aug. 2020, doi: 10.1038/s41397-019-0144-7.

[16] S. A. Smith *et al.*, "Expression and enzyme activity of cytochrome P450 enzymes CYP 3A4 and CYP 3A5 in human skin and tissue-engineered skin equivalents," *Experimental Dermatology*, vol. 27, no. 5, pp. 473–475, May 2018, doi: 10.1111/exd.13483.
[17] Y. Pan, C. E. Ong, Y. F. Pung, and J. Y. Chieng, "The current understanding of the interactions between nanoparticles and cytochrome P450 enzymes – a literature-based review," *Xenobiotica*, vol. 49, no. 7, pp. 863–876, Jul. 2019, doi: 10.1080/00498254.2018.1503360.
[18] S. Cho and Y.-R. Yoon, "Understanding the pharmacokinetics of prodrug and metabolite," *Transl Clin Pharmacol*, vol. 26, no. 1, p. 1, 2018, doi: 10.12793/tcp.2018.26.1.1.
[19] A. Sereemaspu, P. Hongpitich, R. Rojanathan, P. Maneewatta, S. Ekgasit, and W. Warisnoich, "Inhibition of Human Cytochrome P450 Enzymes by Metallic Nanoparticles: A Preliminary to Nanogenomics," *International J. of Pharmacology*, vol. 4, no. 6, pp. 492–495, Oct. 2008, doi: 10.3923/ijp.2008.492.495.
[20] W. Warisnoich, P. Hongpitich, and S. Lawanprase, "Alteration in Enzymatic Function of Human Cytochrome P450 by Silver Nanoparticles," *Research J. of Environmental Toxicology*, vol. 5, no. 1, pp. 58–64, Jan. 2011, doi: 10.3923/rjet.2011.58.64.
[21] J. Yang *et al.*, "Oral administration of nano-titanium dioxide particle disrupts hepatic metabolic functions in a mouse model," *Environmental Toxicology and Pharmacology*, vol. 49, pp. 112–118, Jan. 2017, doi: 10.1016/j.etap.2016.12.006.
[22] S. Imai *et al.*, "Size and surface modification of amorphous silica particles determine their effects on the activity of human CYP3A4 in vitro," *Nanoscale Res Lett*, vol. 9, no. 1, p. 651, Dec. 2014, doi: 10.1186/1556-276X-9-651.
[23] J. Lee, J. L. Beers, R. M. Geffert, and K. D. Jackson, "A Review of CYP-Mediated Drug Interactions: Mechanisms and In Vitro Drug-Drug Interaction Assessment," *Biomolecules*, vol. 14, no. 1, p. 99, Jan. 2024, doi: 10.3390/biom14010099.
[24] J. V. Castell, R. Jover, C. P. Martnez-Jimnez, and M. J. Gmez-Lechn, "Hepatocyte cell lines: their use, scope and limitations in drug metabolism studies," *Expert Opinion on Drug Metabolism & Toxicology*, vol. 2, no. 2, pp. 183–212, Apr. 2006, doi: 10.1517/17425255.2.2.183.
[25] M. Chalak *et al.*, "Cell Immortality: In Vitro Effective Techniques to Achieve and Investigate Its Applications and Challenges," *Life*, vol. 14, no. 3, p. 417, Mar. 2024, doi: 10.3390/life14030417.
[26] Y. T. Ung, C. E. Ong, and Y. Pan, "Current High-Throughput Approaches of Screening Modulatory Effects of Xenobiotics on Cytochrome P450 (CYP) Enzymes," *High-Throughput*, vol. 7, no. 4, p. 29, Sep. 2018, doi: 10.3390/ht7040029.
[27] M. Martignoni, G. M. M. Groothuis, and R. De Kanter, "Species differences between mouse, rat, dog, monkey and human CYP-mediated drug metabolism, inhibition and induction," *Expert Opinion on Drug Metabolism & Toxicology*, vol. 2, no. 6, pp. 875–894, Dec. 2006, doi: 10.1517/17425255.2.6.875.
[28] H.-J. Huang, Y.-H. Lee, Y.-H. Hsu, C.-T. Liao, Y.-F. Lin, and H.-W. Chiu, "Current Strategies in Assessment of Nanotoxicity: Alternatives to In Vivo Animal Testing," *IJMS*, vol. 22, no. 8, p. 4216, Apr. 2021, doi: 10.3390/ijms22084216.
[29] M. T. Donato and M. J. Gómez-Lechón, "Fluorescence-Based Screening of Cytochrome P450 Activities in Intact Cells," in *Cytochrome P450 Protocols*, vol. 987, I. R. Phillips, E. A. Shephard, and P. R. Ortiz De Montellano, Eds., in Methods in Molecular Biology, vol. 987. , Totowa, NJ: Humana Press, 2013, pp. 135–148. doi: 10.1007/978-1-62703-321-3_12.
[30] L. Bell *et al.*, "Evaluation of Fluorescence- and Mass Spectrometry–Based CYP Inhibition Assays for Use in Drug Discovery," *SLAS Discovery*, vol. 13, no. 5, pp. 343–353, Jun. 2008, doi: 10.1177/1087057108317480.
[31] L. Chowdhury, "Investigating the size dependent toxicological effect of zinc oxide nanoparticles on Caenorhabditis elegans and the inhibitory potential on cytochrome P450 isozymes," University of Nottingham Malaysia, Selangor, Malaysia. [Online]. Available: https://eprints.nottingham.ac.uk/77199/7/Lamia_Chowdhury_MPhil_Thesis_2024.pdf
[32] S. Y. M. Lim, J. S. E. Loo, M. Alshagga, M. A. Alshawsh, C. E. Ong, and Y. Pan, "In vitro and In silico studies of interactions of cathinone with human recombinant cytochrome P450 CYP(1A2),

CYP2A6, CYP2B6, CYP2C8, CYP2C19, CYP2E1, CYP2J2, and CYP3A5," *Toxicology Reports*, vol. 9, pp. 759–768, 2022, doi: 10.1016/j.toxrep.2022.03.040.

[33] M. J. Akhtar, H. A. Alhadlaq, A. Alshamsan, M. A. Majeed Khan, and M. Ahamed, "Aluminum doping tunes band gap energy level as well as oxidative stress-mediated cytotoxicity of ZnO nanoparticles in MCF-7 cells," *Sci Rep*, vol. 5, no. 1, p. 13876, Sep. 2015, doi: 10.1038/srep13876.

[34] G. S, A. Belay, C. Reddy Ar, and B. Z, "Synthesis and Characterizations of Zinc Oxide Nanoparticles for Antibacterial Applications," *J Nanomed Nanotechnol*, vol. s8, 2017, doi: 10.4172/2157-7439.S8-004.

[35] M. Deodhar *et al.*, "Mechanisms of CYP450 Inhibition: Understanding Drug-Drug Interactions Due to Mechanism-Based Inhibition in Clinical Practice," *Pharmaceutics*, vol. 12, no. 9, p. 846, Sep. 2020, doi: 10.3390/pharmaceutics12090846.

[36] F. Islam *et al.*, "Exploring the Journey of Zinc Oxide Nanoparticles (ZnO-NPs) toward Biomedical Applications," *Materials*, vol. 15, no. 6, p. 2160, Mar. 2022, doi: 10.3390/ma15062160.

[37] X.-F. Zhang, Z.-G. Liu, W. Shen, and S. Gurunathan, "Silver Nanoparticles: Synthesis, Characterization, Properties, Applications, and Therapeutic Approaches," *IJMS*, vol. 17, no. 9, p. 1534, Sep. 2016, doi: 10.3390/ijms17091534.

[38] C. Wang *et al.*, "Effects of Long-Term Exposure to Zinc Oxide Nanoparticles on Development, Zinc Metabolism and Biodistribution of Minerals (Zn, Fe, Cu, Mn) in Mice," *PLoS ONE*, vol. 11, no. 10, p. e0164434, Oct. 2016, doi: 10.1371/journal.pone.0164434.

[39] R. Gupta and H. Xie, "Nanoparticles in Daily Life: Applications, Toxicity and Regulations," *J Environ Pathol Toxicol Oncol*, vol. 37, no. 3, pp. 209–230, 2018, doi: 10.1615/JEnvironPatholToxicolOncol.2018026009.

[40] J. Jeevanandam, A. Barhoum, Y. S. Chan, A. Dufresne, and M. K. Danquah, "Review on nanoparticles and nanostructured materials: history, sources, toxicity and regulations," *Beilstein J. Nanotechnol.*, vol. 9, pp. 1050–1074, Apr. 2018, doi: 10.3762/bjnano.9.98.

[41] L. Kumar, P. Kumar, A. Narayan, and M. Kar, "Rietveld analysis of XRD patterns of different sizes of nanocrystalline cobalt ferrite," *Int Nano Lett*, vol. 3, no. 1, p. 8, Dec. 2013, doi: 10.1186/2228-5326-3-8.

[42] S.-W. Bian, I. A. Mudunkotuwa, T. Rupasinghe, and V. H. Grassian, "Aggregation and Dissolution of 4 nm ZnO Nanoparticles in Aqueous Environments: Influence of pH, Ionic Strength, Size, and Adsorption of Humic Acid," *Langmuir*, vol. 27, no. 10, pp. 6059–6068, May 2011, doi: 10.1021/la200570n.

[43] Y. Han *et al.*, "Aggregation and dissolution of ZnO nanoparticles synthesized by different methods: Influence of ionic strength and humic acid," *Colloids and Surfaces A: Physicochemical and Engineering Aspects*, vol. 451, pp. 7–15, Jun. 2014, doi: 10.1016/j.colsurfa.2014.03.030.

[44] S. Aykul and E. Martinez-Hackert, "Determination of half-maximal inhibitory concentration using biosensor-based protein interaction analysis," *Analytical Biochemistry*, vol. 508, pp. 97–103, Sep. 2016, doi: 10.1016/j.ab.2016.06.025.

[45] K. A. Bachmann and J. D. Lewis, "Predicting Inhibitory Drug—Drug Interactions and Evaluating Drug Interaction Reports Using Inhibition Constants," *Ann Pharmacother*, vol. 39, no. 6, pp. 1064–1072, Jun. 2005, doi: 10.1345/aph.1E508.

[46] B.-F. Krippendorff, P. Lienau, A. Reichel, and W. Huisinga, "Optimizing Classification of Drug-Drug Interaction Potential for CYP450 Isoenzyme Inhibition Assays in Early Drug Discovery," *SLAS Discovery*, vol. 12, no. 1, pp. 92–99, Feb. 2007, doi: 10.1177/1087057106295897.

[47] R. Attaallah and A. Amine, "The Kinetic and Analytical Aspects of Enzyme Competitive Inhibition: Sensing of Tyrosinase Inhibitors," *Biosensors*, vol. 11, no. 9, p. 322, Sep. 2021, doi: 10.3390/bios11090322.

[48] R. Ramsay and K. Tipton, "Assessment of Enzyme Inhibition: A Review with Examples from the Development of Monoamine Oxidase and Cholinesterase Inhibitory Drugs," *Molecules*, vol. 22, no. 7, p. 1192, Jul. 2017, doi: 10.3390/molecules22071192.

[49] K. Delaune and K. Alsyouri, "Physiology, Non-competitive Inhibitor. [Updated 2022 Sep 12]," in *StatPearls [Internet]*, treasure Islan (FL), 01012024. [Online]. Available: https://www.ncbi.nlm.nih.gov/books/NBK545242/

[50] L. Z. Benet, J. K. Sodhi, G. Makrygiorgos, and A. Mesbah, "There is Only One Valid Definition of Clearance: Critical Examination of Clearance Concepts Reveals the Potential for Errors in Clinical Drug Dosing Decisions," *AAPS J*, vol. 23, no. 3, p. 67, May 2021, doi: 10.1208/s12248-021-00591-z.

[51] E. Fröhlich, T. Kueznik, C. Samberger, E. Roblegg, C. Wrighton, and T. R. Pieber, "Size-dependent effects of nanoparticles on the activity of cytochrome P450 isoenzymes," *Toxicology and Applied Pharmacology*, vol. 242, no. 3, pp. 326–332, Feb. 2010, doi: 10.1016/j.taap.2009.11.002.

[52] J. G. Lamb, L. B. Hathaway, M. A. Munger, J. L. Raucy, and M. R. Franklin, "Nanosilver Particle Effects on Drug Metabolism In Vitro," *Drug Metab Dispos*, vol. 38, no. 12, pp. 2246–2251, Dec. 2010, doi: 10.1124/dmd.110.035238.

[53] D.-Z. Tu *et al.*, "Reversible and Irreversible Inhibition of Cytochrome P450 Enzymes by Methylophiopogonanone A," *Drug Metab Dispos*, vol. 49, no. 6, pp. 459–469, Jun. 2021, doi: 10.1124/dmd.120.000325.

[54] D. A. Rock and L. C. Wienkers, "Characterization of Cytochrome P450 Mechanism Based Inhibition," in *Drug Metabolism Handbook*, 1st ed., A. F. Nassar, P. F. Hollenberg, J. Scatina, S. Kanti Manna, and S. Zeng, Eds., Wiley, 2022, pp. 465–526. doi: 10.1002/9781119851042.ch15.

[55] M. J. Limo *et al.*, "Interactions between Metal Oxides and Biomolecules: from Fundamental Understanding to Applications," *Chem. Rev.*, vol. 118, no. 22, pp. 11118–11193, Nov. 2018, doi: 10.1021/acs.chemrev.7b00660.

[56] W. Jiang, K. Yang, R. W. Vachet, and B. Xing, "Interaction between Oxide Nanoparticles and Biomolecules of the Bacterial Cell Envelope As Examined by Infrared Spectroscopy," *Langmuir*, vol. 26, no. 23, pp. 18071–18077, Dec. 2010, doi: 10.1021/la103738e.

[57] Z. Yang and C. Xie, "Zn2+ release from zinc and zinc oxide particles in simulated uterine solution," *Colloids and Surfaces B: Biointerfaces*, vol. 47, no. 2, pp. 140–145, Feb. 2006, doi: 10.1016/j.colsurfb.2005.12.007.

[58] M. Seray, A. Skender, and A. S. Hadj-Hamou, "Kinetics and mechanisms of Zn2+ release from antimicrobial food packaging based on poly (butylene adipate-co-terephthalate) and zinc oxide nanoparticles," *Polym. Bull.*, vol. 78, no. 2, pp. 1021–1040, Feb. 2021, doi: 10.1007/s00289-020-03145-z.

[59] W. T. Tadesse, E. M. Mlugu, W. Shibeshi, W. A. Degu, E. Engidawork, and E. Aklillu, "CYP3A and CYP2B6 Genotype Predicts Glucose Metabolism Disorder among HIV Patients on Long-Term Efavirenz-Based ART: A Case-Control Study," *JPM*, vol. 12, no. 7, p. 1087, Jun. 2022, doi: 10.3390/jpm12071087.

[60] L. Wang and G.-H. Du, "Paclitaxel," in *Natural Small Molecule Drugs from Plants*, Singapore: Springer Singapore, 2018, pp. 537–543. doi: 10.1007/978-981-10-8022-7_89.